Biochimica et Biophysica Acta 1808 (2011) 1888–1895

Contents lists available at ScienceDirect

Biochimica et Biophysica Acta

journal homepage: www.elsevier.com/locate/bbamem

A CRAC-like motif in BAX sequence: Relationship with protein insertion and pore activity in liposomes

Eduardo Martínez-Abundis [a], Francisco Correa [a], Emma Rodríguez [b], Elizabeth Soria-Castro [c], José S. Rodríguez-Zavala [a], Diana Pacheco-Alvarez [d], Cecilia Zazueta [a,*]

[a] Departamento de Bioquímica, Instituto Nacional de Cardiología, I.Ch., 14080, D.F., Mexico
[b] Laboratorio de Biología Celular. Departamento de Fisiología, Instituto Nacional de Cardiología, I.Ch., 14080, D.F., Mexico
[c] Departamento de Patología, Instituto Nacional de Cardiología, I. Ch., 14080, D.F., Mexico
[d] Escuela de Medicina, Universidad Panamericana, México 03920, D.F., Mexico

ARTICLE INFO

Article history:
Received 6 May 2010
Received in revised form 26 January 2011
Accepted 21 March 2011
Available online 5 April 2011

Keywords:
Bax
Cholesterol
CRAC motif

ABSTRACT

Several proteins that interact with cholesterol have a highly conserved sequence, corresponding to the cholesterol recognition/interaction amino acid consensus. Since cholesterol has been proposed to modulate both oligomerization and insertion of the pro-apoptotic protein BAX, we investigated the existence of such a motif in the BAX sequence. Residues 113 to 119 of the recombinant BAX α5-helix, **LFY**FAS**K**, correspond with the sequence motif described for the consensus pattern, –L/V-(X)(1–5)-Y-(X)(1–5)-R/K. Functional characterization of the point mutations, K119A, Y115F, and L113A in BAX, was performed in liposomes supplemented with cholesterol, comparing binding, integration, and pore forming activities. Our results show that the mutations Y115F and L113A changed the cholesterol-dependent insertion observed in the wild type protein. In addition, substitutions in the BAX sequence modified the concentration dependency of carboxyfluorescein release in liposomes, although neither pore activity of the wild type or of any of the mutants significantly increased in cholesterol-enriched liposomes. Thus, while it is likely that the putative CRAC motif in BAX accounts for its enhanced insertion in cholesterol-enriched liposomes; the pore forming properties of BAX did not depend on cholesterol content in the membranes, albeit those mutations changed the pore channeling activity of the protein.

1. Introduction

BAX is a pro-apoptotic member of the Bcl-2 protein family that normally resides in an inactive state in the cytoplasm of normal cells. After an apoptotic stimulus, BAX undergoes conformational changes [1–4], becoming a mediator of the intrinsic phase of apoptosis by its insertion into mitochondrial membranes, a process that culminates in release of cytochrome c and activation of effector caspases [5]. One of the proposed mechanisms that accounts for such an effect is that oligomeric BAX forms pores in the outer mitochondrial membrane [6], while a second proposal states that BAX induces the opening of the permeability transition pore (mPTP), inducing mitochondrial swelling, rupture of the outer membrane, and cytochrome c release [7]. Both mechanisms are not necessarily mutually exclusive.

There are evidences that emphasize the importance of the Bcl-2 family protein interactions with and within membranes. It is known, for example, that members of the Bcl-2 family interact with mitochondrial contact sites [8,9] and induce remodeling of mitochondrial membranes [10,11]. Lucken-Ardjomande et al. demonstrated that cholesterol inhibits BAX activation and oligomerization, although BAX insertion into the cholesterol-enriched membranes was slightly increased [12]. Conversely, other groups have shown that cholesterol reduces the ability of BAX to change from a membrane-associated protein to a membrane-integral protein. Interestingly, an increased binding, but a reduced insertion of BAX, has been observed when cholesterol was added to liposomes or mitochondrial membranes [13]. Recently, we demonstrated that cholesterol depletion from isolated mitochondria confers resistance to mPTP opening induced by recombinant BAX [14] and that endogenous BAX is distributed preferentially within mitochondrial fractions enriched with cholesterol and ceramide in the ischemic-reperfused heart [15].

Although it remains unclear how the conformational rearrangements of BAX are regulated to finally lead to its location within mitochondrial membranes, the above findings strongly suggest that cholesterol or other lipids participate in such processes. In this regard, it has been reported that several proteins that interact with cholesterol have an amino acid sequence that is highly conserved and corresponds to the pattern –L/V-(X)(1–5)-Y-(X)(1–5)-R/K, in which (X)(1–5) represents between one and five residues of any

Abbreviations: mPTP, mitochondrial permeability transition pore; CRAC, cholesterol recognition/interaction amino acid consensus

* Corresponding author. Tel.: +52 55 5573 2911 1465; fax: +52 55 5573 0926.
E-mail address: azazuetam@yahoo.com (C. Zazueta).

0005-2736/$ – see front matter © 2011 Elsevier B.V. All rights reserved.
doi:10.1016/j.bbamem.2011.03.008

amino acid [16]. Therefore, in this work, BAX sequence analysis led us to propose the existence of a putative cholesterol recognition/interaction amino acid consensus (CRAC motif) at the α5-helix. We obtained recombinant BAX mutants in the CRAC motif and determined their binding, integration, and pore-forming activity in liposomes supplemented with cholesterol.

2. Materials and methods

Chemicals were of reagent or higher grade from Sigma-Aldrich (St. Louis, MO, USA), unless otherwise specified. GST-sepharose, thrombin protease, and enhanced chemiluminescence system detection were obtained from Millipore (Bedford, MA, USA); protease inhibitors set was from Roche (Germany); anti-BAX monoclonal antibody (Clone 6A7) was from Alexis Biochemicals (Axxora, CA, USA), and conjugated secondary antibodies were from Zymed Laboratories (San Francisco, CA, USA). Carboxyfluorescein was from Molecular Probes (Carlsbad, CA, USA). Type IV-soybean asolectin containing 25% of phosphatidylcholine (PC), cardiolipin (Card), and cholesterol (Chol) were from Sigma-Aldrich (St. Louis, MO, USA).

2.1. Site-directed mutagenesis

QuickChange site-directed mutagenesis kit from Stratagene (San Diego, CA, USA) was used to make point mutations in the putative CRAC motif of recombinant BAX. Briefly, synthetic oligonucleotide primer pairs containing L113A, Y115F, and K119A point mutations, each complementary to the opposing strand of the vector, were extended during temperature cycling by PfuTurbo® DNA polymerase that produced mutated plasmids containing staggered nicks. Following temperature cycling, the products were digested with *Dpn* I to select for mutation-containing synthesized DNA. The nicked vectors were transformed into *Escherichia coli*. The purified plasmid sequences were analyzed at the DNA Sequence Center of the Biotechnology Institute (National Autonomous University of Mexico, UNAM). All genes were entirely sequenced on each strand to verify that additional mutations had not been introduced by the PCR amplification.

2.2. Purification of BAX-ΔC (BAX) protein and BAX mutants

Recombinant GST-BAX-ΔC (protein lacking the C-terminal 20 amino acids) and mutants were prepared according to Xie et al. with slight modifications [17]. Briefly, *E. coli* BL21(DE3)pLysS cells carrying the plasmid pGEX-4T1-BAX-ΔC were grown at 37 °C in Luria broth medium supplemented with 100 μg/ml ampicillin, 25 μg/ml chloramphenicol, and 1% glucose, until OD_{550} was around 0.8. Then, 0.4 mM isopropyl-β-D-thyogalactopiranoside (IPTG) was added and the cells were cultured overnight at 25 °C. The harvested cells were disrupted with lysozyme in the presence of 1% TX100 and sonicated in a saline-phosphate buffer (PBS), pH 7.4. Unbroken cells were eliminated after centrifugation at 5000*g*, for 10 min. A high speed centrifugation (100,000*g* for 30 min at 4 °C) was performed to clear the supernatant, before glutathione-sepharose affinity chromatography. Unbound protein was extensively washed using PBS, pH 7.4, supplemented with 0.1% TX100 and the protein was recovered by overnight proteolytic cleavage with thrombin at room temperature. Eluted BAX was dialyzed against 250 volumes of 10 mM Tris/HCl (pH 8.0), 1 mM EDTA, and 0.1% (v/v) 2-β-mercaptoethanol. BAX was aliquoted and stored at −70 °C.

2.3. BAX oligomerization

BAX oligomerization was induced by incubating the protein with 1% octylglucoside for 60 minutes at 4 °C and then diluted 10 times in the assay buffer.

2.4. Liposomes formation

The lipids were mixed at the ratio 80:12:8 (PC:Card:Chol), dried under a nitrogen stream, and suspended in PBS, pH 7.4, at a final concentration of 2.5 mg p.l./ml. Liposomes without cholesterol were supplemented with Type IV-soybean asolectin containing 25% of phosphatidylcholine (PC) to maintain the same lipid concentration: 88:12 (PC:Card).

We used a modification of the freeze–thaw sonication (F/T/S) method developed by Kasahara and Hinckle [18] and Pick [19], in all experiments. After sonication, the liposomes were frozen and thawed five times, followed by a final brief sonication to re-organize the membranes. The activated protein was incubated with the liposomes at the indicated concentration for 1 h under constant agitation. Then, the samples were diluted 15-fold and centrifuged at 100,000*g* for 45 min. The pellets were suspended in 200 μl of PBS, pH 7.4. The freezing and thawing process was used to rupture and re-fuse the small unilamellar vesicles formed by sonication and to increase the size of the vesicles. For the pore-forming experiments, 800 μl of liposomes were mixed with 200 μl of 20 mM carboxyfluorescein after sonication and then frozen and thawed during five cycles. The number of freeze–thawing cycles was fixed by measuring the increment in fluorescence under different conditions. The liposomes were sonicated briefly after the last freeze–thaw cycle, centrifuged at 100,000*g* during 45 min, washed, and carefully suspended in 200 μl of PBS, pH 7.4. We also performed experiments in liposomes prepared by extrusion with membranes of 0.2 μm size pore. Although liposomes obtained by this method were 80% homogeneous unilamellar structures (independently of cholesterol content), with an average size between 150 and 250 nm (Supplementary Figure S1), they were smaller than those obtained by the freeze/thaw/sonication method (0.5–4.4 μm) (Supplementary Figure S2). The fluorescence of the liposome populations obtained by extrusion was very low, probably due to the size of the vesicles, precluding the comparison of membrane surface changes after the reconstitution experiments.

2.5. BAX insertion into cholesterol-enriched liposomes

BAX insertion into liposomes was evaluated by western blot, using a primary monoclonal anti-BAX antibody (1 μg/ml). Alkaline phosphatase conjugated secondary antibodies were used followed by an enhanced chemiluminescence system detection. Liposomes (1 mg) in 0.5 ml PBS, pH 7.4, were incubated with recombinant BAX at the indicated concentration for 10 min at room temperature. At this point, aliquots were withdrawn from the reconstitution mixture, mixed with sample buffer for electrophoresis, loaded onto SDS-PAGE gels and stained to verify that protein content was the same in both preparations (not shown).

To discard the protein loosely bound to the membranes, the liposomes were incubated with 0.1 M Na_2CO_3, pH 11.5 (alkaline extraction), for 10 min more at room temperature. Then, the liposomes were diluted 10-fold with PBS, pH 7.4, and recovered by centrifugation at 100,000*g* for 45 min. The pellets were suspended in sample buffer for electrophoresis, loaded onto SDS-PAGE gels and transferred to PVDF membranes for immunodetection using anti-BAX monoclonal antibodies. In some experiments, SDS-resistant BAX oligomers were disrupted by treating the samples with trifluoroacetic acid, as described by Sagné et al. [20]. Briefly, BAX samples containing SDS were treated with anhydrous trifluoroacetic acid (TFA) in a 5:1 (v/v) ratio during 15 h and then analyzed by SDS-PAGE.

2.6. Effect of BAX interaction on the fluorescence of liposomes determined by flow cytometry

To get further information on the effects of mutation of the conserved amino acids L113A, Y115F, and K119A on BAX interaction

with liposomes, we analyzed the fluorescence of the liposomes by flow cytometry [21]. Briefly, changes in the mean fluorescence of liposomes with incorporated wild type BAX and mutants were analyzed by using a Beckton Dickinson FACSCalibur Flow Cytometer. Ten thousand liposomes were analyzed using Cell Quest Software at FL1 compensation of 0.8% and a detector compensation threshold FSC-H of E00, with the detectors: FSC of 52 V, SCC of 422 V, and FL1 of 412 V. The particles being illuminated one at a time by different lasers were defined by its granularity (complexity) and by size. In general, the sideward scatter of laser light (SSC) define the granularity and internal complexity of the sample, while the forward scatter (FSC) of laser light is measured to define the size of the particle. Settings for sideward scatter (SSC) were optimized as the noise did not exceed the first log scale, while settings for the forward scatter (FSC) maximized the particle count within a detectable range. The emitted fluorescence was filtered to reach the detector channel (FL1). We assumed that changes in the mean fluorescence of the samples represent membrane surface changes, resulting from protein binding, as reported by Temmerman and Nickel [22]. Results represent changes in mean fluorescence, as analyzed by Kolmogorov–Smirnov statistics.

2.7. Carboxyfluorescein release from cholesterol-enriched liposomes

Liposomes (50–100 μg of p.l.) with entrapped carboxyfluorescein were added to a medium containing 2 ml of phosphate-saline buffer, pH 7.4. Initial fluorescence, corresponding to vesicle entrapped self-quenched fluorescent probe (F_o) was determined at $\lambda_{em} = 488$ and $\lambda_{ex} = 520$ in each single trace. Then, the same concentrations of BAX_{WT} or BAX mutants were used to induce carboxyfluorescein release. At the end of the experiment, 0.05% of TX100 was added to obtain maximal fluorescence (F_{max}). Data are expressed as $\%F = [(F_t - F_o)/F_{max} - F_o] \times 100$, where F_t is the increase in fluorescence after 5 min of BAX addition. F_t values were measured after 5 min of incubation of the vesicles, as maximal response was obtained at this time using BAX wild type.

2.8. Docking model of cholesterol into BAX α-5 helix

Three-dimensional models of wild type mouse BAX and mutants L113A, Y115F and K119A, were obtained with the SWISS-MODEL software (http://www.swissmodel.expasy.org/) [23,24], using the crystal structure reported for BAX from *Homo sapiens* (BAX; accession number 1F16) as template [25]. Then, the α-5 helix region of BAX was taken out from the structure by the use of SPDBV software (http://www.expasy.org/spdbv/) for docking analysis. The models and the molecule of cholesterol for docking were prepared using the software ADT 1.5.2 [26]. Docking of the BAX wild type and mutants with cholesterol was performed using Autodock 4 (http://www.autodock.scripps.edu/) [27]. For docking analysis the α5-helix was set as rigid and cholesterol molecule was set flexible leaving the 6 bonds capable to rotate as active torsions. One hundred conformations were obtained and clustered for the analysis and two families of conformations with different orientation with respect to the α-helix were obtained. The conformation showing the lowest values of binding energy and K_d for each family was represented in the docking model of cholesterol into BAX α5-helix (Fig. 6). Analysis of the resulting structures and generation of figures was performed with PyMOL (http://www.pymol.sourceforge.net/).

2.9. Statistical analysis

Values are means ± SD and were evaluated by one-way ANOVA and Tukey's multiple comparative test. $P \leq 0.05$ was considered the threshold for statistical significance among the indicated groups.

3. Results

3.1. Mutations in the putative CRAC motif of BAX

Residues 113 to 119 of the BAX α5-helix (107-GRVVA**L**F**Y**-FAS**K**LVL) correspond with the sequence motif described for the cholesterol recognition/interaction amino acid consensus pattern, –L/V-(X)(1–5)-Y-(X)(1–5)-R/K. In Table 1, the alignment of amino acid sequences of different proteins is compared: PBRs in the cholesterol recognition region, P450sccs in the region of substrate recognition, other proteins that interact with cholesterol, a segment of the caveolin sequence, and the putative cholesterol binding domain in BAX sequence. To test the hypothesis that this sequence corresponds to a CRAC motif, we modified the three conserved amino acids of the domain. Mutations were introduced by PCR; leusine-113 and lysine-119 were changed to the uncharged residue alanine, and tyrosine-115 was changed to phenylalanine: L113A, Y115F, and K119A (Fig. 1).

3.2. BAX mutants insertion into liposomes

Hydrophobic domains previously folded back within the protein are known to be exposed by non-ionic detergent treatment, inducing BAX oligomerization. Octylglucoside (1%) was incubated with BAX_{WT} and the mutants. The oligomerized state was preserved after SDS-PAGE and, only under extremely de-aggregating conditions, the monomeric form was recovered. Fig. 2A shows the formation of SDS-resistant BAX oligomers of BAX_{WT} and its dissociation with trifluoroacetic acid (TFA). It also shows that the mutants retained the oligomerization properties of BAX_{WT}, after non-ionic detergent activation (Fig. 2B).

Next, we determined the effect of the putative consensus CRAC motif included in the BAX_{WT} sequence and the affinity of this protein to cholesterol, by measuring the insertion of the wild type protein into liposomes without cholesterol and into liposomes supplemented with cholesterol. According to Ardail et al. [28], cholesterol content in the outer membrane represents 7.1 in percent by weight of total lipids; in that work, the outer membrane contact sites were found to possess a higher ratio of cholesterol/phospholipid than the inner membrane contact sites. In our experiments, cholesterol is expected to be distributed randomly along the liposome membrane, thus we decided to use cholesterol at 8% in weight of total lipids. BAX_{WT} association (binding) into the membranes was the same in both types of liposomes; however, after ionic detachment with Na_2CO_3, it was observed that BAX_{WT} maintained stronger interaction with

Table 1
Putative cholesterol recognition/interaction amino acid consensus pattern in different cholesterol-interacting proteins.

Mouse PBR	**147-** ATV**L**N**Y**YVW**R**DNS
Rat PBR	**147-**ATM**L**N**Y**YVW**R**DNS
Human PBR	**147-**ATT**L**N**Y**CVW**R**DN
Rat P450scc	**86-**PW**V**AYHQ**Y**YQ**R**PIG
Human P456scc	**86-**PW**V**AYHQ**Y**YQ**R**PIG
Bovine P450scc	**86-**PW**V**AYHZH**Y**Q**K**PVG
Mouse apolipoprotein A-I	**207-**NPT**L**NE**Y**HT**R**AK
Streptococcus cholesterol oxidase	**417-**ETW**V**SL**Y**LAIT**K**NP
Nocardia cholesterol dehydrogenase	**89-**AS**V**TEA**Y**RQ**R**SFA
Human bile-salt-activated-lipase	**222-**SLQT**L**SP**Y**NKGLI**R**RI
Rabbit acyl-CoA cholesterol acyltransferase	**93-**ST**L**VVD**Y**IDEG**R**LV
Human caveolin	**91-**TFT**V**TK**Y**WFY**R**
Mouse BAX	**109-**VVA**L**F**Y**FAS**K**LVL

Alignment of amino acid sequences of different PBRs in the cholesterol recognition region; P450sccs in the region corresponding to substrate recognition site 1; and proteins that interact with cholesterol (obtained from Genebank), containing the cholesterol recognition/interaction amino acid consensus pattern -L/V-(X)1–5-Y-(X)1–5-R/K-. A possible CRAC motif in BAX sequence located in α5-helix is also shown. The conserved amino acids of sequence motif are highlighted and printed over a gray background. Modified from Li et al., (2001) Proc. Natl. Acad. Sci. USA. 98: 1267–1272.

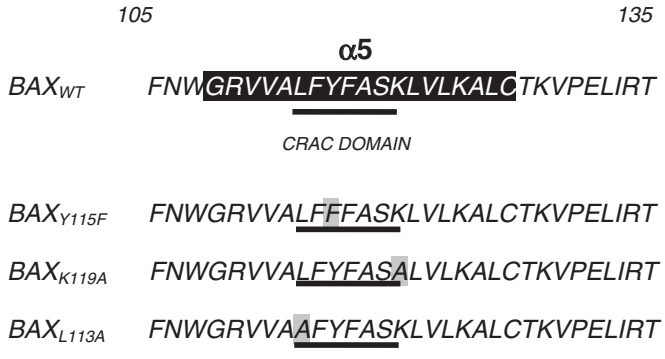

Fig. 1. Partial sequence of the CRAC motif in BAX wild type and mutants. The fragment from residues 105 to 135 of mouse BAX is shown, which includes residues of the α-5 helix, according to TopPred II (Claros and von Heijne), highlighted in white over a black background. Aligned are the sequences of the studied mutants, residues substituted with respect to the wild-type sequence are printed over a light grey background.

cholesterol-enriched liposomes (Fig. 2C). Our interpretation is that a weak association between BAX and lipids occurs preferentially along the membrane in liposomes without cholesterol. Conversely, the BAX proteins that interact with cholesterol in the membrane would be tightly bounded and become more resistant to ionic removal from liposomes enriched with cholesterol. By these reasoning we concluded that in such liposomes, a stronger interaction of BAX avoids Na_2CO_3 detachment from the membrane.

The cholesterol-dependent insertion of the mutants was also analyzed. Results were expressed in percentages to normalize the chemiluminescence signal in each blot, for each peptide, and to eliminate background differences between individual plates, or possible changes in the recognition response of the antibody to each peptide.

The cholesterol-dependent insertion increment observed in the wild type, although less impressive, was maintained in the mutant K119A, but was not observed in either Y115F or L113A mutant. Both of them showed similar insertion into liposomes regardless of the cholesterol content (Fig. 3). Thus, while it is likely that cholesterol plays a role in BAX$_{WT}$ and K119A mutant insertion, this behavior is reduced in mutants Y115F and L113A.

3.3. Membrane surface effects in liposomes induced by interactions between lipids and BAX

In the absence of protein, the vesicles showed different mean fluorescence values, depending on the presence of cholesterol. In

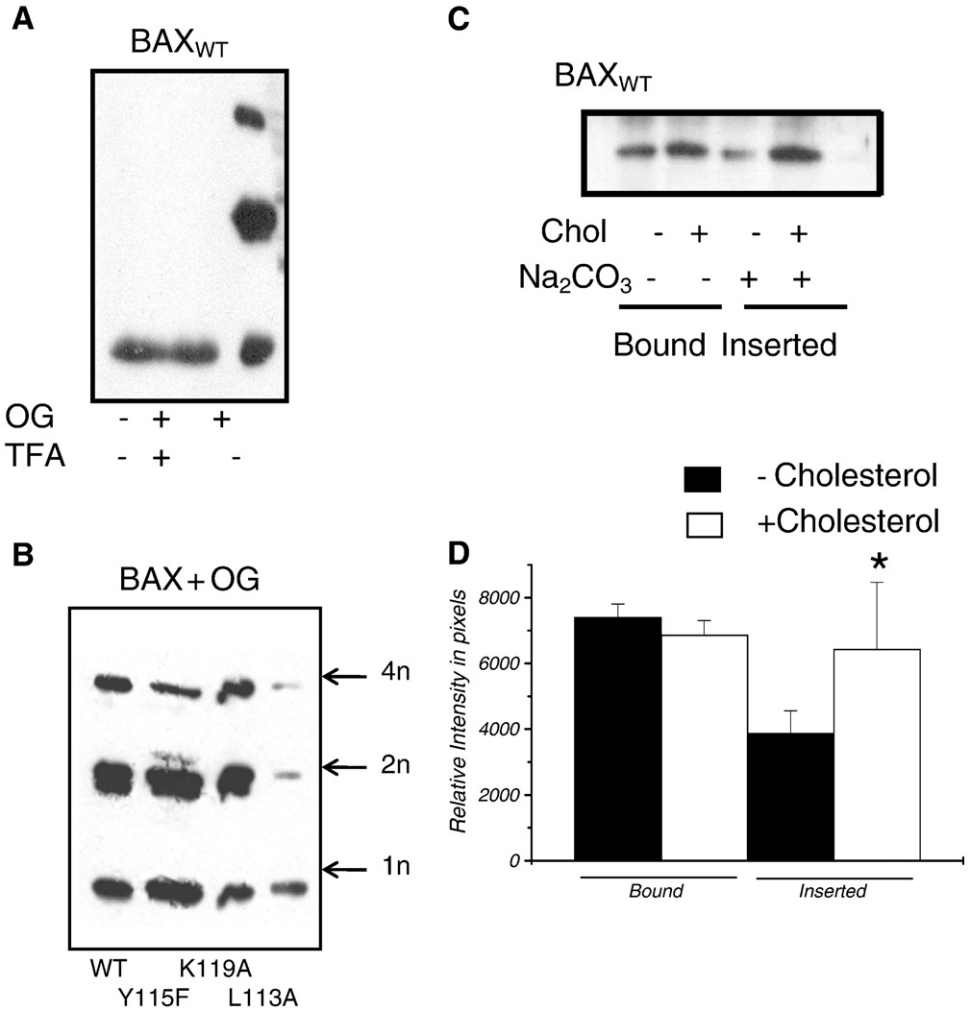

Fig. 2. Cholesterol increases BAX$_{WT}$ insertion into liposomes. Representative immunoblots showing the dissociation of BAX$_{WT}$ oligomers after TFA treatment (A), and BAX mutants oligomerization properties (B). Panel C shows BAX$_{WT}$ reconstitution into liposomes enriched with cholesterol without any treatment (bound) and after alkaline extraction with Na_2CO_3. The liposomes were incubated with 0.1 M Na_2CO_3, pH 11.5 (alkaline extraction), for 10 min more at room temperature. Then, the liposomes were diluted 10-fold with PBS, pH 7.4, and recovered by centrifugation at 100,000*g* for 45 min. The pellets were suspended in sample buffer for electrophoresis, loaded onto SDS-PAGE gels and transferred to PVDF membranes for immunodetection using anti-BAX monoclonal antibodies. A representative immunoblot and the histogram quantification (Panel D) of three experiments with different preparations are shown. (*$P \leq 0.05$ vs. BAX$_{WT}$ insertion in liposomes without cholesterol).

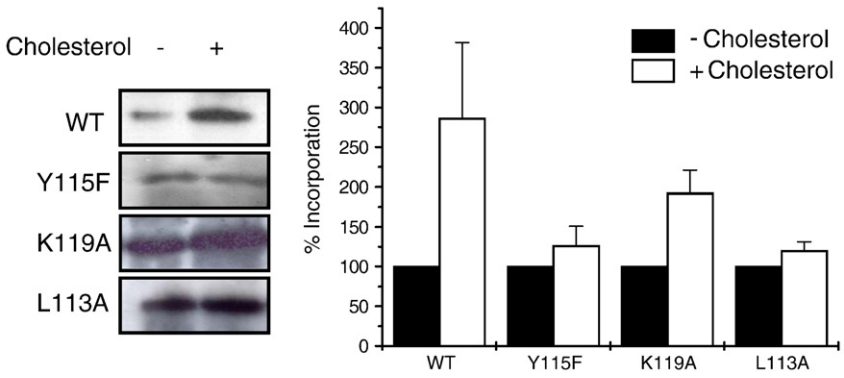

Fig. 3. BAX mutants insertion into liposomes enriched with cholesterol. Left panel: Representative immunoblots of BAX_{WT}, Y115F, K119A, and L113A insertion into PC:Card and PC:Card:Chol liposomes. Right panel: Histogram plots showing quantification of three different immunoblots. BAX_{WT} and mutants immunodetection in liposomes without cholesterol was normalized as 100% and compared to the signal obtained in cholesterol-enriched liposomes for each protein. ($^*P \leq 0.05$).

Fig. 4A, it is shown that the mean fluorescence was lower in liposomes enriched with cholesterol, suggesting variations in bilayer complexity. Accordingly, changes in mean fluorescence within each type of liposomes promoted by BAX_{WT} and mutants interaction were evaluated. In Fig. 4B it is shown that BAX_{WT} and all mutants diminished significantly the mean fluorescence of PC:Card liposomes ($D = 0.12$ to 0.20 at $P \leq 0.001$). Conversely, in PC:Card:Chol liposomes, BAX_{WT} and L113A mutant, promoted an increase in the mean fluorescence of the vesicles ($D = 0.1$ and $D = 0.06$ respectively), whereas the mean fluorescence in liposomes with reconstituted Y115F and K119A was lower than that observed in the liposomes without protein ($D = 0.06$–0.07 at $P \leq 0.001$). From results shown in Figs. 3 and 4, we concluded that Tyr115 is more relevant to cholesterol-dependent insertion of BAX, than Leu113 or Lys119.

3.4. Effect of cholesterol on pore formation by BAX mutants in liposomes

Activated BAX_{WT} induced carboxyfluorescein (CF) leakage in both types of liposomes. This concentration-dependent release was slightly enhanced in cholesterol-enriched liposomes (Fig. 5A), possibly reflecting the favored insertion of the protein when cholesterol is a component of the bilayer (Fig. 3). All the mutants induced a

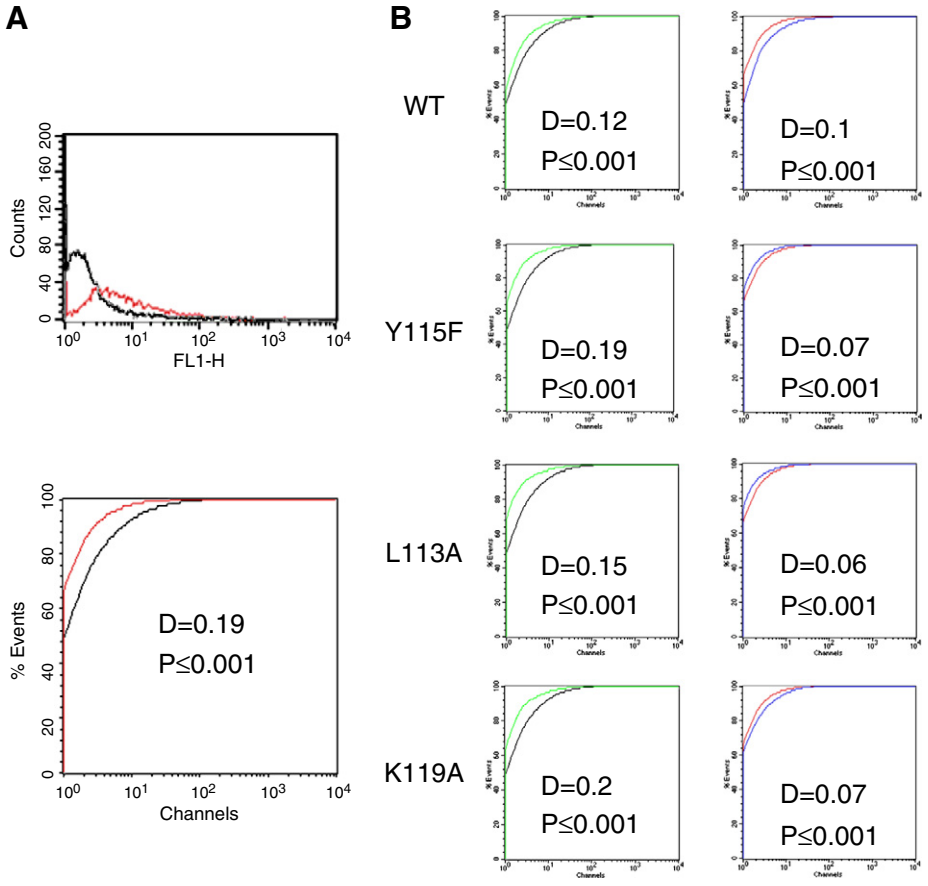

Fig. 4. Flow cytometric analysis of interactions between liposome lipids and BAX wild type and mutants. (Panel A) Histogram overlay and mean fluorescence of the vesicle population of PC:Card (black) and PC:Card:Chol (red) liposomes calculated by Kolmogorov–Smirnov statistical analysis in absence of protein. (Panel B) Mean fluorescence changes after protein interaction in PC:Card (green) and PC:Card:Chol (blue) liposomes. D, refers to the difference on a logarithmic scale between liposomal populations at $P \leq 0.001$. $\lambda Ex = 530$ nm and $\lambda Em = 488$ nm.

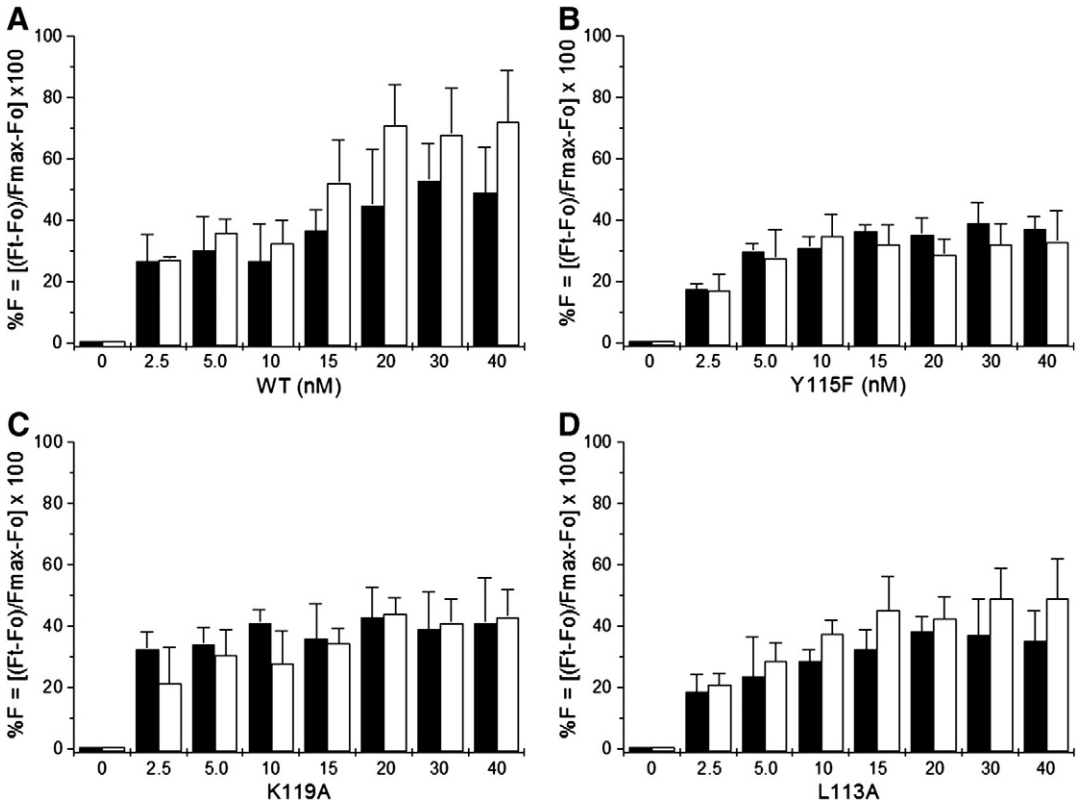

Fig. 5. Carboxyfluorescein release from liposomes enriched with cholesterol induced by BAX_{WT} and mutants. Liposomes (50–100 μg lipids) with entrapped carboxyfluorescein were added to a phosphate-saline buffer, pH 7.4. The fluorescent probe release was induced by adding the indicated BAX_{WT} and mutant concentrations. Data represent the mean ± S.D. of three different experiments; black bars, liposomes without cholesterol; white bars, liposomes enriched with cholesterol.

diminished carboxyfluorescein leakage as compared with the wild type (Fig. 5B, C and D). Fluorescence release at 40 nM concentration was 32% in Y115F; 42% in K119A and 49% in L113A versus 70.8% induced by the wild type protein in cholesterol-enriched liposomes. This suggests that although mutations of the putative CRAC motif in BAX have no effect on the oligomerization properties of the protein (Fig. 2B), the resulting structures have a diminished efficiency in forming a pore, as compared with the wild type protein.

3.5. Docking model of cholesterol into a CRAC motif signature included in BAX α-5 helix

The α5-helix conformation of BAX_{WT} containing the CRAC domain was analyzed in light of the crystal structure reported for BAX from *Homo sapiens.* According to previous reports, the transmembrane domain of BAX is predicted to form a helix from residue 108 up to 126 [29,30]. Multiple conformations of cholesterol into the putative CRAC motif in BAX_{WT} α5-helix were analyzed with Autodock 4. The docking analysis of cholesterol with BAX_{WT} α5-helix rendered two main families of conformations, which account for the accommodation of cholesterol (Fig. 6). Conformations with the lower binding constants and lower binding energies for each family (K_d = 50.6 μM, −5.86 kCal/mol and K_d = 43.2 μM, −5.95 kCal/mol) were selected (Table 2). The conformations in which the cholesterol molecule fits into two possible cavities were defined arbitrarily as "**a**" and "**b.**" In the first cavity, formed by A112, L113, and F116, the small polar head of cholesterol could be located, close to R109 in the **a** conformation. The second groove (**b** conformation) is formed by Y115, F116, and L120 (Fig. 6) with the 3'OH group of cholesterol facing the opposite side of BAX structure. Docking analysis was also carried out with the BAX mutants (Supplementary Figure S5). For all mutants the values of binding energy as well as K_d were increased in both cholesterol conformations (Table 2). Interestingly, mutants Y115F and L113A showed the highest increase in binding energy and K_d for both conformations, consistent with the diminution on cholesterol-dependent insertion into the membrane of these mutants (Fig. 3), compared to BAX_{WT}.

4. Discussion

The hypothesis that Bcl-2 family members are activated and dock at the mitochondrial outer membrane in response to a particular membrane environment has been proposed by different research groups. For example, Kim et al. showed that tBid binds to cardiolipin at the mitochondrial contact sites [31]. Another report indicates that cardiolipins are essential for α-6 helix tBid binding, and that both electrostatic interactions and lipid organization play a crucial role for tBid to penetrate into the membrane [32,33]. Cardiolipin is also relevant for BAX activation and for binding of the first helix of the protein to the mitochondrial membrane [34]. In this context, results from our laboratory showed coexistence in mitochondrial detergent-resistant membranes (MDRM) of BAX and cholesterol, along with contact sites forming proteins, e.g. ANT and VDAC. We also observed that cholesterol extraction from mitochondrial membranes, promoted a marked diminution in BAX insertion and inhibition of cytochrome c release. Accordingly, we proposed that modifications in the cholesterol content could lead to alterations in the physical environment of the membrane, consequently changing the chance of certain proteins to partition into cholesterol enriched domains [15].

To this respect, it is known that some proteins share a common amino acid consensus pattern that favors their association with cholesterol. This domain consists of a neutral and hydrophobic amino acid, such as leucine or valine, a neutral and polar amino acid, like tyrosine, and a basic amino acid, such as arginine or lysine. It has been proposed that leucine or valine would interact with the hydrophobic side chain of cholesterol, whereas tyrosine would interact with the polar 3'OH-group of cholesterol and arginine or lysine may help to

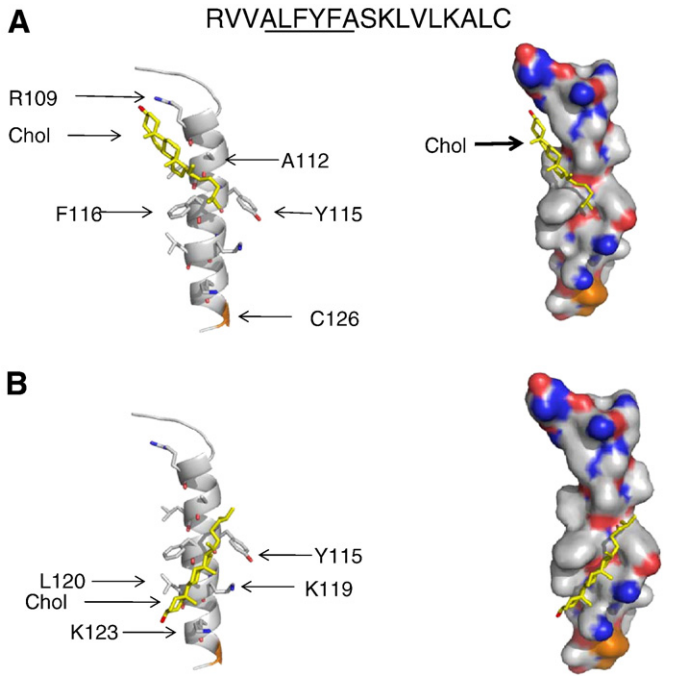

Fig. 6. Docking of cholesterol on helix α-5 of BAX. Alpha-5 helix of BAX, which contains the putative CRAC domain, was used to develop a model of possible interactions with cholesterol (yellow). In A and B, it is shown the ribbon presentation of the helix, with the side chain of some amino acids represented as sticks of the two most favored conformations of cholesterol found by docking (lowest K_d and binding energy values) and the surface representations of the same helix. It can be appreciated that the side chain of the amino acids in the helix form a groove into which cholesterol fits. Figures were prepared using PyMOL, as described under Materials and methods. Arrows indicate the position of important amino acids presented as one letter symbols. The complete sequence of the helix is depicted on the top of the figure and the CRAC domain is shown highlighted.

create a pocket [16]. Our results with recombinant BAX protein show that mutations in Tyr115 and Leu113 changed the cholesterol-dependent insertion observed in the wild type protein by western blot analysis (Fig. 3), whereas fluorescence changes exerted by BAX_{WT} in cholesterol-enriched liposomes were higher than those promoted by the mutants (Fig. 4). Besides, the pore properties of the mutants diminished as compared to the wild type, independently from the cholesterol content in the membranes. However, the release of the entrapped substrate showed a tendency to increase in cholesterol-enriched liposomes at least in the wild type (Fig. 5).

In a putative CRAC motif, the side-chains of aromatic amino acids would facilitate interaction with the relatively flat structure of cholesterol. After clustering analysis, we obtained two conformations with the lowest energy (K_d) for cholesterol docking into BAXα5-helix.

Table 2
Values of binding energy and K_d obtained from the docking of cholesterol on α-5 helix of BAX_{WT} and the different mutants.

BAX	Cholesterol alignment*	Binding energy (kCal)	K_d (μM)
WT	a	−5.86	50.6
	b	−5.95	43.2
Y115F	a	−5.67	70.4
	b	−5.58	81.2
K119A	a	−5.82	54.1
	b	−5.38	113.2
L113A	a	−5.23	146.8
	b	−5.38	113.1

* a and b refer to the two families of conformations found in the docking analysis and represent the conformation of lowest energy of binding and K_d for each family. These conformations are shown in Fig. 6 and Supplemental Figure 5.

In one of them, cholesterol is located close to Arg109 in the α-5 helix of BAX_{WT}, and the groove could be formed by Leu113, Tyr115, and Phe116 (Fig. 6A, B). Tyr115 could interact with the side chain of Lys119, stabilizing the caveat. By eliminating the reactive group in the Y115F mutation, this stabilization could be lost, partially explaining the difference in the insertion properties between this mutant and the wild type. As for L113A, the insertion properties were also modified, although no relevant changes were observed in the mean fluorescence of liposomes after reconstitution.

In a second favorable conformation, the cavity could be formed by Tyr115, Leu119, and Lys120 (Fig. 6C and D), albeit, in this conformation, the only possible interaction of the cholesterol polar group would be with Lys123. In contrast with other proposals, as those reported for the CRAC motif of the peripheral-type benzodiazepine receptor [35] and for HIV gp41 peptides [36], our model does not support critical interactions of the central tyrosine residue with the cholesterol hydroxyl group. In such models, electrostatic and hydrophobic interactions between the central tyrosine in the motif and cholesterol are possibly due to the location of this residue in the boundary region of the membrane interface.

We are aware of the limitations of the proposed model, as the water-soluble structure used here is the only one structure available for BAX. However, we used this structure as the docking target for our study, as it has been predicted that the first fragment of the hairpin of BAX, namely α -helices 5 and 6, has a predominantly α-helical structure in lipid-mimetic and lipid environments [37]. Thus, this model should be taken cautiously as it only represents an illustration of the possible interactions of the peptides with cholesterol, but that behavior could be different in the membrane. Considering that in the formation of a pore, several BAX molecules must be involved, the polar residues imbibed into the lipid belayed could be interacting with charged residues of other BAX molecules to stabilize the oligomer in the membrane, thus substitutions in the peptide structure could account for reduced efficiency in pore formation and in consequently in pore activity.

Variable effects of mutants on mean liposome fluorescence open the possibility that the presence of a CRAC sequence could be only one of multiple factors that contribute to enhance protein binding into cholesterol-rich domains. A good example of the aforementioned is caveolin, which possesses a CRAC sequence and also has three palmitoyl groups [38,39]. Among the different proteins associated to a CRAC motif, caveolin constitutes a *bona fide* marker for a type of cholesterol-rich domain in biological membranes. Epand et al. studied segments of this protein that correspond to a CRAC motif. Although these peptides promote the segregation of cholesterol into domains from mixtures of the sterol with phosphatidylcholine, the authors concluded that the presence or absence of a CRAC motif is not a sufficient criterion to determine the extent to which a protein will promote the segregation of cholesterol in membranes [40].

As mentioned above, other features that promote the partition of proteins into cholesterol-rich domains are certain types of lipidation. In this sense, Sakurai et al. described post-transcriptional myristoylation in tBid [41], however, mutations of the myristoylation site in tBid, which indeed suppress myristoylation capabilities, do not affect the interaction of tBid with mitochondria. Although it is known that palmitoylated proteins are generally found in the raft fraction of membranes enriched with cholesterol [42], there are no evidences of such post-translational modifications in BAX structures. Another explanation of our results, besides the possible structural features already mentioned, could be the existence of interactions or conformations in the intact oligomeric protein that could not be reproduced in our experimental design. Indeed, there are reports that segments in gp41 proteins, which do not have formally a CRAC sequence, are also likely targeted to raft domains [43].

Summarizing, our experiments add new information to the possible components of the machinery of BAX membrane

permeabilization mechanism. Beyond the proposal that the critical event for BAX membrane permeabilization function is the transition from a membrane-integrated 'monomer' to a detergent-resistant oligomeric form [44], we propose that the insertion mechanism involves lipid organization in the membrane and that a sequence that corresponds to a cholesterol recognition/interaction amino acid consensus motif in BAX contributes to the incorporation of proteins into cholesterol-enriched membranes, although this interaction could be increased by other factors.

Supplementary materials related to this article can be found online at doi:10.1016/j.bbamem.2011.03.008.

Acknowledgments

We greatly acknowledge the generous gift of pGEX-4T-I BAX plasmid from Dr. John Reed (Burnham Institute for Medical Research, La Jolla, CA) and Rocío Torrico Lavayen for technical assistance. This work was partially supported by grant 80791-M to C.Z. from the National Council of Science and Technology (CONACYT), Mexico. The authors state no conflict of interest.

References

[1] A. Schinzel, T. Kaufmann, M. Schuler, J. Martinalbo, D. Grubb, C. Borner, Conformational control of Bax localization and apoptotic activity by Pro168, J. Cell Biol. 164 (2004) 1021–1032.
[2] J. Yethon, R. Epand, B. Leber, R. Epand, D.W. Andrews, Interaction with a membrane surface triggers a reversible conformational change in Bax normally associated with induction of apoptosis, J. Biol. Chem. 278 (2003) 48935–48941.
[3] V. Mikhailov, M. Mikhailova, K. Degenhard, M.A. Venkatachalam, E. White, P. Saikumar, Association of Bax and Bak Homo-oligomers in Mitochondria. Bax Requirement for Bak reorganization and cytochrome c release, J. Biol. Chem. 278 (2003) 5367–5376.
[4] P.F. Cartron, C. Moreau, L. Oliver, E. Mayat, K. Meflah, F.M. Vallette, Involvement of the N-terminus of Bax in its intracellular localization and function, FEBS Lett. 512 (2002) 95–100.
[5] B. Antonsson, Bax and other pro-apoptotic Bcl-2 family "killer-proteins" and their victim the mitochondrion, Cell Tissue Res. 306 (2001) 347–361.
[6] O. Terrones, B. Antonsson, H. Yamaguchi, H.G. Wang, J. Liu, R.M. Lee, A. Herrmann, G. Basañes, Lipidic pore formation by the concerted action of proapoptotic Bax and tBid, J. Biol. Chem. 279 (2004) 30081–30091.
[7] M. Narita, S. Shimizu, T. Ito, T. Chittenden, R.J. Lutz, H. Matzuda, Y. Tsujimoto, Bax interacts with the permeability transition pore to induce permeability transition and cytochrome c release in isolated mitochondria, Proc. Natl Acad. Sci. U.S.A. 95 (1998) 14681–14686.
[8] M. Lutter, M. Fang, X. Luo, M. Nishijima, X. Xie, X. Wang, Cardiolipin provides specificity for targeting of tBid to mitochondria, Nat. Cell Biol. 2 (2000) 754–761.
[9] M. Lutter, G.A. Perkins, X. Wang, The pro-apoptotic Bcl-2 family member tBid localizes to mitochondrial contact sites, BMC Cell Biol. 2 (2001) 22–30.
[10] L. Scorrano, M. Ashiya, K. Buttle, S. Weiler, S.A. Oakes, C.A. Mannella, S.J. Korsmeyer, A distinct pathway remodels mitochondrial cristae and mobilizes cytochrome c during apoptosis, Dev. Cell 2 (2002) 55–67.
[11] R.F. Epand, J.C. Martinou, M. Fornallaz-Mulhauser, D.W. Hughes, R.M. Epand, The apoptotic protein tBid promotes leakage by altering membrane curvature, J. Biol. Chem. 277 (2002) 32632–32639.
[12] S. Lucken-Ardjomande, S. Montessuit, Bax activation and stress-induced apoptosis delayed by the accumulation of cholesterol in mitochondrial membranes, Cell Death Differ. 15 (2008) 484–493.
[13] E. Christenson, S. Merlin, M. Saito, P. Schlesinger, Cholesterol effects on Bax pore activation, J. Mol. Biol. 381 (2008) 1168–1183.
[14] E. Martínez-Abundis, N. García, F. Correa, M. Franco, C. Zazueta, Changes in specific lipids regulate BAX-induced mitochondrial permeability transition, FEBS J. 274 (2007) 6500–6510.
[15] E. Martínez-Abundis, F. Correa, N. Pavón, C. Zazueta, Bax distribution into mitochondrial detergent-resistant microdomains is related to ceramide and cholesterol content in post-ischemic hearts, FEBS J. 276 (2009) 5579–5588.
[16] H. Li, V. Papadopoulos, Peripheral-type benzodiazepine receptor function in cholesterol transport, Endocrinology 139 (1998) 4991–4997.
[17] Z. Xie, S. Schendel, S. Matsuyama, J. Reed, Acidic pH promotes dimerization of Bcl-2 family proteins, Biochemistry 37 (1998) 6410–6418.
[18] M. Kasahara, P. Hinckle, Reconstitution of D-glucose transport catalyzed by a protein fraction from human erythrocytes in sonicated liposomes, Proc. Natl Acad. Sci. U.S.A. 73 (1976) 396–400.
[19] U. Pick, Liposomes with a large trapping capacity prepared by freezing and thawing of sonicated phospholipid mixtures, Arch. Biochem. Biophys. 212 (1981) 186–194.
[20] C. Sagné, M.F. Isambert, J.P. Henry, B. Gasnier, SDS-resistant aggregation of membrane proteins: application to the purification of the vesicular monoamine transporter, Biochem. J. 316 (1996) 825–831.
[21] C. Zazueta, J. Ramírez, N. García, I. Baeza, Cardiolipin regulates the activity of the reconstituted mitochondrial calcium uniporter by modifying the structure of the liposome bilayer, J. Membr. Biol. 191 (2003) 113–122.
[22] K. Temmerman, W. Nickel, A novel flow cytometric assay to quantify interactions between proteins and membrane lipids, J. Lipid Res. 50 (2009) 1245–1254.
[23] M. Peitsch, M. Wilkins, L. Tonella, J. Sánchez, R. Appel, D. Hochstrasser, Large-scale protein modelling and integration with the SWISS-PROR and SWISS-2PAGE databases: the example of *Escherichia coli*, Electrophoresis 18 (1997) 498–501.
[24] K. Arnold, L. Bordoli, J. Kopp, T. Schwede, The SWISS-MODEL workspace: a web-based environment for protein structure homology modeling, Bioinformatics 22 (2006) 195–201.
[25] M. Suzuki, R.J. Youle, N. Tjandra, Structure of Bax: coregulation of dimer formation and intracellular localization, Cell 103 (2000) 645–654.
[26] S.A. Sanner, Python: a programming language for software integration and development, J. Mol. Graph. Mod. 17 (1999) 57–61.
[27] R. Huey, G.M. Morris, A.J. Olson, D.S. Goodsell, A semiempirical free energy force field with charge-based desolvation, J. Comput. Chem. 28 (2007) 1145–1152.
[28] D. Ardail, J.P. Privats, M. Egret-Charlierg, C. Levratg, F. Lerme, P. Louisot, Mitochondrial contact sites. Lipid composition and dynamics, J. Biol. Chem. 265 (1990) 18797–18802.
[29] A. García-Sáez, I. Mingarro, E. Pérez-Payá, J. Salgado, Membrane-insertion fragments of Bcl-x_L, Bax Bid Biochem. 43 (2004) 10930–10943.
[30] A. García-Sáez, M. Coraiola, M. Dalla-Serra, I. Mingarro, P. Müller, J. Salgado, Peptides corresponding to helices 5 and 6 of Bax can independently form large lipid pores, FEBS J. 273 (2006) 971–981.
[31] T. Kim, Y. Zhao, W. Ding, J. Shin, X. He, Y. Seo, J. Chen, H. Rabinowich, A. Amoscato, X. Yin, Bid-cardiolipin interaction at mitochondrial contact site contributes to mitochondrial cristae reorganization and cytochrome C release, Mol. Biol. Cell 15 (2004) 3061–3072.
[32] P.X. Petit, P. Dupaigne, F. Pariselli, F. Gonzalvez, F. Etienne, C. Rameau, S. Bernard, Interaction of the alpha-helical H6 peptide from the pro-apoptotic protein tBid with cardiolipin, FEBS J. 276 (2009) 6338–6354.
[33] F. Gonzalvez, F. Pariselli, O. Jalmar, P. Dupaigne, F. Sureau, M. Dellinger, E. Hendrickson, S. Bernard, P.X. Petit, Mechanistic issues of the interaction of the hairpin-forming domain of tBid with mitochondrial cardiolipin, PLoS ONE 5 (2010) e9342.
[34] M.A. Sani, E.J. Dufourc, G. Gröbner, How does the Bax-α1 targeting sequence interact with mitochondrial membranes? The role of cardiolipin, Biochim. Biophys. Acta 1788 (2009) 623–631.
[35] N. Jamin, J.M. Neumann, M.A. Ostuni, T.K. Vu, Z.X. Yao, S. Murail, J.C. Robert, C. Giatzakis, V. Papadopoulos, J.J. Lacapère, Characterization of the cholesterol recognition amino acid consensus sequence of the peripheral-type benzodiazepine receptor, Mol. Endocrinol. 19 (2005) 588–594.
[36] R.F. Epand, A. Thomas, R. Brasseur, S.A. Vishwanathan, E. Hunter, R.M. Epand, Juxtamembrane protein segments that contribute to recruitment of cholesterol into domains, Biochemistry 16 (2006) 6105–6114.
[37] A.J. García-Saez, M. Coraiola, M. Dalla Serra, I. Mingarro, G. Menestrina, J. Salgado, Peptides derived from apoptotic Bax and Bid reproduce the poration activity of the parent full-length proteins, Biophys. J. 88 (2005) 3976–3990.
[38] C. Le Lan, J. Gallay, M. Vincent, J.M. Neumann, Structural and dynamic properties of juxta-membrane segments of caveolin-1 and caveolin-2 at the membrane interface, Eur. Biophys. J. 39 (2010) 307–325.
[39] E. Spisni, V. Tomasi, A. Cestaro, S. Tosatto, Structural insights into the function of human caveolin, Biochem. Biophys. Res. Comm. 338 (2005) 1383–1390.
[40] R. Epand, B.G. Sayer, R.F. Epand, Caveolin scaffolding region and cholesterol-rich domains in membranes, J. Mol. Biol. 345 (2005) 339–350.
[41] N. Sakurai, K. Moriya, T. Suzuki, K. Sofuku, H. Mochiki, O. Nishimura, T. Utsumi, Detection of co- and posttranslational protein N-myristoylation by metabolic labeling in an insect cell-free protein synthesis system, Anal. Biochem. 362 (2007) 236–244.
[42] H. Shogomori, A.T. Hammond, A.G. Ostermeyer-Fay, D.J. Barr, G.W. Feigenson, E. London, D.A. Brown, Palmitoylation and intracellular domain interactions both contribute to raft targeting of linker for activation of T cells, J. Biol. Chem. 280 (2005) 18931–18942.
[43] R.M. Epand, Do proteins facilitate the formation of cholesterol-rich domains? Biochim. Biophys. Acta Biomembr. 1666 (2004) 227–238.
[44] M.G. Annis, E.L. Soucie, P.G. Dlugosz, J.A. Cruz-Aguado, L.Z. Penn, B. Leber, D.W. Andrews, Bax forms multispanning monomers that oligomerize to permeabilize membranes during apoptosis, EMBO J. 24 (2005) 2096–2103.